PSFC/RR-05-1

Simulation of Hydrogen Generation from Methane Partial Oxidation in a Plasma Fuel Reformer

N. Margarit Bel[1], J.B. Heywood[1], L. Bromberg[2]

January 7, 2005

[1] MIT Department of Mechanical Engineering and Sloan Automotive Laboratory
[2] MIT Plasma Science and Fusion Center

ABSTRACT

A model for the chemistry in a plasma fuel reformer or plasmatron has been developed. The plasma fuel reformer is set up to produce syngas (hydrogen and carbon monoxide gas mixture) from partial oxidation of hydrocarbons. The behavior of methane as fuel has been investigated to characterize and simulate the plasmatron performance. The goal of this work has been improved understanding of the physical/chemical processes within the reactor. The simulation tool used was CHEMKIN 3.7, using the GRI methane combustion mechanism. The Partially Stirred Reactor application (PASR) simulates random mixing by a frequency mixing parameter, which is directly dependant of the system fluid dynamic properties. The fuel reformer was designed as a reactor where combustion is initiated by an electric discharge due to ohmic heating of the arc region. From discharge observations, energy estimations and model simulations, it was found that the electric arc initiates combustion by locally raising the temperature and then propagating the reaction by heat and mass transfer/mixing to the surroundings. Simulation results demonstrated that there is an optimum characteristic mixing time for each residence time, depending on the initial temperature reached at the arc. It was also found that for given power input into the system, the more spread the energy is, or the more mass is heated to a moderate temperature, the better the calculated performance.

Keywords: methane, partial oxidation, fuel reformation, hydrogen

I. INTRODUCTION

Hydrogen (H_2) as fuel has a very high flame speed. When mixed with other fuels, hydrogen addition increases flame speed and improves engine combustion stability (Tully, 2002). Due to higher flame stability for fuel-H_2 mixtures, engines can burn mixtures with low fuel content (ultra-lean conditions) without misfire. Due to leaner operation, combustion occurs at more moderate temperatures. When having lower combustion temperatures, the engine will produce less NO_x, since nitric oxide formation is directly related to temperature conditions (Bromberg *et al*, 2000). Ultra lean operation allows operation with reduced vacuum in the cylinder, reducing the throttling losses in the engine.

The presence of carbon monoxide (CO) in addition to pure hydrogen has been proved to be beneficial in H_2-enhanced engines (Topinka, 2003). The CO-H_2 mixture helps inhibit knock by slowing the autoignition reactions and by accelerating the flame speed. CO has chemical energy content that can be combusted into CO_2 releasing heat and also be counted as a dilutant in terms of lean operation. An engine working with H_2 addition can be redesigned to have a higher compression ratio and increased manifold pressure, because of the high octane of the hydrogen rich gas addition. Thus, high fuel efficiency can be achieved by the combined use of ultra lean operation, high compression and turbo-charged, with possibility of engine downsizing at constant peak power.

One of the main obstacles to H_2 gas addition is the difficulty of handling and storage of hydrogen. Generating H_2 onboard of vehicles enables the use of hydrogen gas addition for ICE use. The process of fuel reformation by partial oxidation process is basically burning a hydrocarbon in a combustor with low content in oxygen or air (very fuel rich conditions). Instead of achieving complete combustion of the hydrocarbon into water and CO_2, a gas mixture of H_2 and CO is produced. This gas mixture is produced onboard a vehicle from gasoline reforming in the plasmatron and routed to the ICE together with more gasoline.

The plasmatron is a small combustor (20 cm to 30 cm long) that requires low electrical power (200 W to 900 W) and uses the same fuel as the engine, producing syngas on demand. It is necessary to understand how the device functions and responds to changes in conditions in order to predict system control issues. Thus, a comprehensive model than may be used to predict and understand the performance of the plasmatron is developed in this paper.

II. SYSTEM DESCRIPTION

Several versions of the plasmatron have been developed. We concentrated our tests to a single setup schematically shown in Figure 1. The main reactor chamber consists of a cylindrically shaped region with two annular electrodes, one on the top, closer to the fuel injector, and one on the bottom, next to the downstream reactor zone. The electrodes are located across a radial air inlet which introduces air with substantial swirl. The zone between the two electrodes is the discharge zone. The discharge starts directly across the electrodes, but the gas flow forces the discharge into the discharge zone. The swirl motion of the air rotates the discharge in the discharge region and the roots of the

discharge on the electrodes. In the discharge zone combustion initiation takes place due to strong heating by the electric discharge.

The system has two main inlet streams: fuel and air, both at ambient temperature. Fuel is pressure-driven and axially injected into the discharge region. There are three reactor inlets for air: premixed with the fuel and axially injected (referred to as Atomization air because that is its purpose in the case of liquid fuels); flowing next to the walls without swirl (Wall protect air); creating swirl in the discharge region (Plasma air). In some experiments, the oxidizer is oxygen enriched air. The fuel mass flow rate varies between 0.5 g/s and 1.0 g/s, while the total air flow rate varies from 30 l/min to 250 l/min at standard conditions. The downstream region is usually wider than the plasma region. It can operate with or without catalyst. The total length of the plasmatron ranges from 25 cm to 30 cm.

III. DISCHARGE PHYSICAL MODEL: OHMIC HEATING

A useful way to examine the arc behavior is to look at its images. A series of movies were taken using a Redlake MASD monochrome high-speed video camera, with up to 12,000 images per second framing capability. An example of arc images in a sequence is shown in Figure 2. Each picture is a view of the discharge zone taken downstream along the plasma reformer axis. These pictures were taken without fuel, so the light seen is a result of the electric discharge. The arc curls, grows and moves around the reactor volume from its start up to its end. The discharge was restriking approximately every 3 ms, and rotates with a 1 ms period.

The figure window size measures 4 cm. Using this scale, we estimated that the average length of the arc is 3.5 cm, growing from 2 cm at start up to 5 cm before extinction. Wider/brighter zones lengths were doubled, since we had no sense of depth from the 2-D image and it is expected that brighter spot correspond to an element in the discharge that has a large axial component. Pictures also showed that the diameter ranges from 0.5 mm to 0.7 mm; thus the volume of the discharge is $7\text{x}10^{-9}$ m^3 to $1\text{x}10^{-8}$ m^3 ($7\mu l$-$10\mu l$).

The plasmatron is driven by an alternating current power supply whose power ranges from 200 W to 900 W. The frequency of the power supply is 200 kHz and the CW voltage varies between 0.6 kV and 0.7 kV. From current and voltage traces measured with the oscilloscope when using a power supply capable of delivering 600 W, the energy delivered through the arc discharge in a given time is integrated, allowing the calculation of the average power on the order of 250 W. This indicates that the power supply system is not ideal, with an approximate delivery efficiency of 50%. In addition, only a fraction of this power is delivered to the gas mixture due to losses to the electrodes. For arc discharges, the total loss to the electrodes due to dissipation in sheaths is estimated to be 50% (Heywood, 1988). This adds up to a total of 75% energy loss from the power supply to the gas mixture. Hence, the real power delivered to the gas is 150 W.

Measurements of the current and voltage traces were recorded with a Tektronics Digital Scope TDS 3032B oscilloscope synchronized with the camera. Figure 3 shows the instantaneous power. From the voltage and current traces we draw a new apparent frequency for the arc strike that is not visible in the movies and is related to the current reversal time. On average, every 0.5 ms the power drops and immediately reappears (Figure 4). The power-measured frequency (2kHz) is considered to correspond to the

different arcs within a same mass, while the visual-measured frequency (350 Hz) is correlated to the residence time of high temperature gas mixture within the arc discharge region.

Assuming an ohmic heating process, the thermal energy delivered to the gas can be calculated from the power input P. The differential temperature increase dT of a specific mass m for each time differential dt is related to the input power by energy-conservation,

$$\eta \cdot P \cdot dt = m \cdot c_p \cdot dT \qquad \text{(Eq. 1)}$$

at constant pressure. The constant pressure heat capacity of the mixture c_p is shown in Figure 5 as a function of temperature. η, the efficiency of ohmic dissipation to thermal energy in the gas is assumed to be 50%, as mentioned above. The mass was determined from the arc volume v (Figure 6), and its density estimated using the equation of state of an ideal gas.

The integration of Equation 1 must be over a time τ, which is the time during which the power is supplied. The discharge duration is ~ 0.5 ms. From discharge visualizations it is determined that the arc extinguishes every 3 ms, which is of the order of the reactor residence time. Whether the discharge duration or the residence time for τ are used will produce very different results. The first hypothesis assumes that the power is supplied through the discharge only for a certain period (from its formation to its breakdown). The second hypothesis assumes that the arc is almost continuous and is heating the same mass of gas during a residence time.

$$\int_\tau \frac{MW \cdot c_p}{T} \cdot dT = \int_\tau \eta \cdot P \cdot \frac{R}{v \cdot p} \cdot dt \qquad \text{(Eq. 2)}$$

The time interval of integration, the power supplied and the volume of the arc were assumed to be 200 W and 9×10^{-9} m^3 respectively. The molecular weight was assumed to be constant and equal to 17 g/mol (Figure 7), and the heat capacity function for the gas mixture was substituted by a 3-step linear correlation (Figure 5).

Alternatively, it is possible to establish a condition where thermal conduction determines the temperature in the discharge, cooled by flowing gas at the discharge boundary. Thermal conduction and convection (Thiele et al., 2002) heat up the gas surrounding the discharge.

Iterating Equation 2 for the final temperature (the initial temperature is set to 300 K) provides us with the temperature increase of the arc due to ohmic heating by the discharge. There are two solution, one for each hypothesis. When assuming the energy release heats up only the arc mass during a period equal to the discharge duration, the temperature increase estimation is of the order of 2,000 K. However, if we consider that the discharge is almost continuous and affects the arc mass for a period equal to its residence time in the reactor, then the gas temperature is of the order of 11,000 K. Both assumptions represent extremes. It is unrealistic to assure that all power is transformed into thermal energy within the arc. Therefore, an intermediate temperature between 2,000 K and 11,000 K is considered to be more realistic. If the heat is limited by thermal

conduction, the value of the central temperature is around 4000 K with an average temperatures of about 2000 K.

The impact of the heating effect and of the plasma generated radicals is discussed next. Several simulations for methane partial oxidation with air have been carried out using the PLUG application of CHEMKIN. This model predicts the evolution of all species involved in a chemical scheme with time, in a homogeneous closed adiabatic system. We used the GRI mechanism for these calculations. The reactants included were methane and air (79% nitrogen and 21% oxygen.), at atmospheric pressure. Initial conditions for the O/C ratio of the inlet reagents were kept constant and equal to 1.

To determine the minimum temperature required for ignition a range of initial temperatures from 300 K to 2,000 K were used in the calculations. Based on the residence time of the total plasmatron (500 ms), a minimum temperature of 1,100 K was necessary for the reaction to start inside the fuel reformer, and a higher temperature was required (1,500 K) for ignition to occur inside the discharge zone (3 ms). The ignition delay was found to decay exponentially with temperature as shown in Figure 8.

The next step consisted of testing the ignition response to seeding the gas flow with radicals (such as OH) or assuming that part of the reactants were partially dissociated into O or H in the plasma zone. It is known that free O radicals, obtained from dissociation of oxygen, are able to start the H_2-O_2 branching mechanism that is responsible for the fuel-air mixture ignition. On the other hand, we can also obtain H radicals from the pyrolysis of methane. OH is an alternative combustion initiation precursor. A possible route for OH generation is through aldehyde formation. All those mechanisms happen at high temperatures (Glassman, 1996).

Ignition delay of combustion was studied for different concentrations of radicals at different initial temperatures. We tested 1%, 10% and 20% dissociation of oxygen into O (which correspond to 0.3%, 2.8% and 5.8% mole fraction of O), and 1%, 10% and 20% dissociation of methane into H and CH_3 (which correspond to 0.3%, 2.7% and 5.6% mole fraction for H and for CH_3), individually and simultaneously combined. Also, we tried seeding with OH radical in fractions of 0.3% and 3% molar.

Table 1 shows a summary of the results obtained. 1% dissociation of the reactants was not sufficient for ignition within the reactor, while 10% dissociation required high initial temperature for ignition to happen within the residence time. At initial temperature higher than 1,000 K, seeding with radicals have a small effect on the ignition delay. Radicals in concentration higher than 3% (20% dissociation) significantly reduced ignition time at 500 K. However, these high concentrations in the plasmatron flow are unrealistic. The necessary amount of energy to convert 10% of the O_2 gas in the reactor into its radicals O (Suris, 1985) is high. Considering that it is necessary to spend 10 eV to generate an O radical (960 kJ/mol), 1 kW would be necessary to dissociate 10% of the oxygen into O for a flow rate of 1 g/s through the plasmatron. This amount of energy is not available. The plasmatron power supply delivers less than 225 W though the arc. Therefore, it is not reasonable that we find radicals concentrations higher than 1% in the plasma region. In conclusion, high temperatures are required for ignition to occur within the plasmatron residence time.

IV. REACTOR CHEMICAL MODEL

To chemically simulate the plasmatron, both a kinetic and a mixing model are needed. A kinetic chemistry model requires a group of reactions individually defined. Each reaction is described by its production rate, which is proportional to the temperature-dependent kinetic rate constant. The most common characterization for the kinetic rate constant follows the Arrhenius scheme. The methane combustion GRI mechanism (Smith et al., 2004) provides all necessary constants for the kinetic mechanism definition.

The mixing model is related to the mean kinetic energy of the flow and how it is transferred to turbulent kinetic energy κ or kappa:

$$\kappa = const \cdot u'^2 \qquad \text{(Eq. 3)}$$

Here u' is the root mean square of velocity fluctuations of the flow, thus kappa is a kinetic energy per unit mass. The turbulent kinetic energy is transferred from eddies of large scales to eddies in microscales, where it will be dissipated by viscous motion. The mixing process in a reactor may be characterized by the mixing frequency τ_{mix}, which is usually modeled by the reciprocal of the turbulence time scale (Komiyama, 1975) or also known as mixing rate intensity β:

$$\tau_{mix} = \frac{1}{\beta} = \frac{L}{u'} \qquad \text{(Eq. 4)}$$

where L is the size of the integral scale. The integral scale is the length scale that establishes the time scale of mixing. Turbulence theory states that the mixing intensity is determined by the integral scale and the energy dissipation rate. Hence now, we define the energy dissipation rate ε (epsilon) as the reciprocal time scale multiplied by the kinetic energy per unit mass:

$$\varepsilon = \frac{u'^3}{L} \qquad \text{(Eq. 5)}$$

We can now derive the following equation:

$$\tau_{mix} = C \cdot \frac{\kappa}{\varepsilon} \qquad \text{(Eq. 6)}$$

The proportionality constant C depends on the flow configuration, and is chosen to be 1 in our calculations. A summary of the analysis of the power input into the reactor is presented in Table 2, which helps us estimate the average $\kappa = 7.40 \times 10^3$ m^2/s^2 as well as the average $\varepsilon = 6.15 \times 10^7$ m^2/s^3 for the system, and thus find $\tau_{mix} = 1.2 \times 10^{-4}$ s.

CFD calculations using FLUENT 6.0 software were performed at the PSFC (Bromberg, 2002) in order to provide the system τ_{mix}. For different flow configurations, but maintaining the same plasmatron design, the estimated values for kappa and epsilon produced a $\tau_{mix} = 1.0 \times 10^{-4}$ s. We conclude that the mixing time is of order hundreds of microseconds.

The PASR of CHEMKIN was used to model the plasmatron reactor physically and chemically (Reaction Design, 2003). Inside the PASR the reagents are imperfectly mixed

at the molecular level, i.e., the reactive fluids are not completely diffused into each other. The composition and temperature in the PASR are described by a probability density function (PDF). Velocity fluctuations are ignored and thus the PDF is over scalars only. The mixing process in the PASR is characterized by the mixing frequency $1/\tau_{mix}$. The PASR does not resolve fluid dynamic details, and therefore the mixing frequency parameter must be prescribed as a user input. The mean reactor residence time and the chemical reaction time are the other two characteristic times of the reactor. τ_{res} is a necessary input for the software. The chemical reaction time τ_{chem} is internally computed from the set of reactions that describe the kinetic mechanism. The results from the PASR approach a perfectly stirred reactor limit when the ratios τ_{mix}/τ_{res} and τ_{mix}/τ_{chem} are significantly smaller than one, or in other words, when the characteristic mixing time is small compared to the other characteristic times, the mixing can be considered to be instantaneous.

The stochastic mixing model represents the composition of the fluid at any position in a reactor as an ensemble of fluid elements which are identified in terms of their individual thermodynamic states. The state of each element may be assumed to be uniform throughout its volume at any instant of time. However, this given state may vary with time as a result of mixing and reaction within the element (Flagan et al., 1973).

A group of N equal mass fluid elements represents the fluid composition. A fraction of these elements, Na/N represents the flow through the fuel atomizer, the remaining N - Na represent the pure combustion air. Each element behaves as a Plug Flow Reactor, which reacts according to the appropriate chemical rate equations during a short time period. After this time period, mixing interactions are computed. The frequency at which elements collide or mix, the mixing time, needs to be determined. At each mixing iteration a group of n elements is chosen at random from the entire ensemble of N. Those chosen elements are mixed by pairs, yielding two new elements of exactly same thermodynamic properties and composition. At any time, the mean composition and other mean properties can be evaluated by taking an average over the N fluid elements. Between mixings, each element will individually experience adiabatic chemistry appropriate to its own conditions. The Monte Carlo integration is usually used to solve the master equations, which include mass conservation, energy conservation and chemical kinetics differential equations (Brown, 1996).

V. RESULTS AND ANALYSIS

The two principal user-set parameters that describe the PASR are the characteristic times: mixing time and residence time. For a plasmatron device working with a flow of 3 g/s of air-fuel mixture the residence time in the discharge zone is estimated to be 1 ms. The mixing time is 0.1 ms.

Based on these values, a series of simulations for methane partial oxidation were carried out. The initial temperature of the high temperature stream (that describes the plasma heated gas) and the fraction of elements at that high temperature were varied to investigate the effects of the arc in the discharge zone and to study the combustion initiation and propagation process in the plasmatron.

As previously discussed, the temperature achieved by the air-fuel mixture was estimated to be between 2,000 and 11,000 K. However, the GRI mechanism thermodynamic data

has been only validated for temperatures up to 5,000 K. Therefore, our first calculations tried to simulate the methane oxidation for an O/C=1, residence time (τ_{res})=1 ms and mixing time (τ_{mix})=0.1 ms, with 1% of the molar flow through the reactor (equivalent to the arc volume) at 5,000 K and the rest of the flow at ambient temperature (300 K). One percent of the flow at high temperature, however, proved insufficient to achieve significant methane conversion into syngas (less than 5%). Combustion was initiated in the hot elements but the energy propagation by mixing with other elements rapidly quenched the chemistry; the number of hot elements was too small compared to the total.

To analyze the system response to a change in the O/C ratio, 10% of the molar flow was set at high temperature (4,000 K) with the same characteristic times as above. Results are shown in Figure 9. Temperature and gas composition at the exhaust of the discharge region are plotted as a function of O/C ratio. The trends show that the more oxygen is present in the flow, the higher the methane conversion is, yielding higher concentration of oxygenated products such as CO, H_2O and CO_2. Hydrogen production stays practically invariable.

For a fraction of hot elements equal to 10% of the molar flow into the plasmatron, the impact on methane conversion of different mixing times was calculated for the same residence time and initial temperatures of the hot elements (varied from 2,000 K to 5,000 K). Figure 10 shows the fraction of hydrogen at the exhaust of the discharge region (τ_{res}=1 ms). Higher initial temperatures for the hot elements yield higher amounts of H_2. In fact, for τ_{mix}=0.01 ms and T=3,000 K for 10% of the elements, the PASR simulation produces as much hydrogen as the experiments performed with the plasmatron (6.5% mole fraction).

There is a optimal mixing/residence time ratio for maximum hydrogen generation for each initial temperature of the hot elements. This maximum moves towards lower mixing times as temperature rises, that is to say, the higher the initial temperature of hot elements, the shorter is the mixing time necessary to reach the hydrogen peak. This phenomenon is explained by quenching. When the mixing process is fast (lower τ_{mix}), the hot elements mix more often and transfer their energy to more elements. Thus, if they have low temperature (2,000 K) and mix rapidly, they lose the ignition potential quicker and fewer non-hot elements can benefit from energy transfer to initiate combustion and produce H_2. At high temperature (5,000 K), more energy is available and therefore more mixes are possible before the hot elements are quenched, allowing short mixing times to enhance methane conversion. For low mixing rates ($\tau_{mix}>\tau_{res}$) and high temperature (5,000 K), combustion kinetics occur faster than mixing and thus the temperature of the hot elements decreases[1] before they are able to initiate combustion in other elements.

To understand why 1% of the molar flow into the plasmatron at high temperature (5,000 K) was not sufficient to propagate combustion to the whole reactor, the impact of changing the fractions of hot elements at different initial temperatures was explored. Figure 11 shows the H_2 concentration with the PASR model for τ_{mix}=0.1 ms and τ_{res}=1 ms. For 1% of the molar flow at hot temperature, none of the initial temperatures tried was enough to generate more than 10% of the experimental production of hydrogen

---

[1]Adiabatic temperature for methane partial oxidation is lower than initial temperature when $T_i>3,000$ K.

(equal to 1% mass fraction). In general, for all the products of combustion, each temperature resulted in a linear dependence of the concentration with hot fraction, up to 10% of hot stream. Again, as temperature increases the concentration of the species increased. This scheme indicates, in general, that increased elements at moderate temperature (3,000 K) can produce as much or more syngas than fewer elements at a higher temperature (5,000 K).

The arc volume is smaller than 1% of the total reactor volume and the temperature reached in the discharge is estimated to be between 2,000 and 11,000 K. However, the simulations indicate that higher fractions of hot stream with lower energy would be more advantageous to methane conversion. A question is thus posed: is the arc heating the same mass for the total discharge duration or is it affecting more mass than the one in the arc volume, and thus heating it up to lower temperatures than the calculated ones? Thiele et al., (2002) did a 2-D study of a spark ignition system in which shows how the hot temperature region is not only limited to the mass within the arc, but that there is also a radial heat transfer by conduction to the surrounding areas that could explain higher fractions of hot elements at temperatures lower than the arc, but still high enough to initiate combustion. This convection process can affect lengths up to 4 times larger than the arc diameter, which would represent that the real arc volume would be 16 times bigger than the estimated by visualization. In that case, the fraction of hot elements at high temperature would be about a 2% of the flow. Nevertheless, the physical model developed for the plasmatron discharge is based on assumptions and further experiments and calculations need to be carried out to validate them.

Species concentration at the exhaust of the discharge zone for the simulation calculations and the plasmatron experiments are compared in Table 4 for methane partial oxidation at O/C=1. The PASR model was set with τ_{mix}=0.1 ms and τ_{res}=1 ms as the closest estimated values to the experimental system. One can observe that the simulation case that matches the hot stream input thermal energy to the electrical power supplied to the discharge in the experiments (300 W) yields lower concentrations for all the syngas species. Using the PASR model, we need to increase the power to almost ten times the power used in the experiment to reach the experimentally measured hydrogen and CO concentrations. Even in that case, water and CO_2 concentrations do not match. The discrepancy between the experimental energy supply for the plasmatron to produce syngas from methane and the amount of energy necessary in the PASR simulations to reach a similar level of methane conversion has yet to be adequately explained. The power requirement to heat the mass within the arc between the tested values 1,000 K and 5,000 K lies in both cases under 500 W. The power required for the PASR simulation to heat 1% of the flow through the plasmatron to the high temperature, is in that range, but the methane conversion is less than 10% of the methane conversion that the experimental results show for the same amount of power. It is necessary to heat up 5% of the flow to 5,000 K to produce the amount of hydrogen that the experiments produce, and this requires 3 kW, much higher than the available power. This energy discrepancy could be explained by the limitations in the PASR model that requires mixture uniformity of the inlet streams. In the experiments, the heterogeneity of the gas within the reactor facilitates combustion of zones in which oxygen concentration is higher even though temperature is lower, releasing extra energy from the exothermic combustion reaction. Indeed, it was determined experimentally that a high level of fuel stratification was required for reforming. The PASR simulation assumes that all non-hot elements initially have the

same relative air/fuel ratio, in other words, the two reactor streams (hot and cold one) are homogeneous and have the same composition. If the element distribution is nonuniform, there are elements in which methane/air ratio is appropriate for combustion, and substantial heat is released in this elements that increase substantially the average temperature, thus increasing the conversion rate (at the expense of some fuel combustion). The chemical energy flow could become the additional energy above the electrical discharge energy necessary to reach the experimentally determined methane conversion. The available PASR model is inadequate to simulate non-uniformity in mixture composition.

Clearly, the PASR model must be further developed so that it better matches the experimental situation. The capability for using a probability distribution profile for variables such as temperature or composition entering the reactor could help reproduce the expected heterogeneity of the real system. However, such a feature is not yet available. Software improvements are needed to model the plasmatron more completely.

VI. CONCLUSIONS

- The temperature rise of the gas mixture within the arc is a direct effect of the power supplied to the discharge and it is necessary for the initiation of the combustion process. Combustion is then propagated by mixing of this hot reacted gas mass with the surrounding mixture. A discharge model that assumes ohmic heating of the gas mixture was used to estimate temperatures between 2,000 K and 11,000 K for the mass within the visible arc region. Radicals generated by the discharge are not the primary ignition trigger of the process. Radical presence helps combustion initiation at temperatures under 1,000 K. However, at the temperatures reached in the arc, above 2,000 K, the radicals effect on ignition is negligible.

- There is an optimum mixing time for each residence time of the plasmatron reactor that depends on the temperature reached at the arc; it is of order of the residence time for 2,000 K and of order 1/100 of the residence time for 5,000 K. There is a quenching effect that shifts this maximum towards lower mixing rates for lower arc gas temperatures (2,000 K). The optimum for higher arc gas temperatures (5,000 K) is of the order of the estimated mixing time for the real plasmatron (0.1 ms) and produces similar methane conversion into syngas than the experiments. The more elements of the PASR at intermediate temperature (3,000 K) simulating the arc, the higher methane conversion. Fewer hot elements at high temperature (5,000 K) provide equal or less syngas production for the same power delivery.

- Non uniformities in relative fuel-air ratio are believed to contribute the additional thermal energy needed to effectively initiate much more complete chemical reaction within the plasmatron. The PASR does not adequately simulate the fuel-air and temperature non uniformities in the experimental plasmatron in the current format. Several modifications that involve the number of streams entering the reactor, heterogeneity of these streams and capability to create a temperature probability distribution profile for these streams could help improve the simulation results.

Acknowledgements

REFERENCES

Bromberg, L., CFD Calculations for the Plasmatron, PSFC Internal Report, 2002.

Bromberg, L., Rabinovich, A., Cohn, D., Heywood, J., "Emissions Reductions Using Hydrogen from Plasmatron Fuel Converters", Diesel Engine Emissions Reduction Workshop, 2000.

Brown, J., *An stochastic Mixing Model for Predicting Emissions in a Direct Injection Diesel Engine*, MIT Ph. D. Thesis in Ocean Engineering, September 1996.

Flagan, R. C., Appleton, P., A Stochastic Model of Turbulent Mixing with Chemical Reaction: Nitric Oxide Formation in a Plug-Flow Burner, MIT, December 1973.

Glassman, I., Combustion, Academic Press, Inc., California, 1996.

Heywood, J. B., Internal Combustion Engine Fundamentals, McGraw-Hill, New York, 1988.

Komiyama, K., *The effects of Fuel Injector Characteristics on Fuel-Air Mixing in a Burner*, MIT Ph. D. Thesis in Mechanical Engineering, January 1975.

Reaction Design, PASR Application User Manual, CHEMKIN Collection 3.7.1, 2003.

Smith, G. P., Golden, D. M., Frenklach, M., Moriarty, N. W., Eiteneer, B., Goldenberg, M., Bowman, C. T., Harnson, R. K., Song, S., Gardiner, W. C., Vitali, V., GRI mechanism 3.0, http://www.me.berkeley.edu/gri_mech/.

Suris, A. L., Handbook of Thermodynamic High Temperature Process Data, Hemisphere Publishing Corporation, Moscow, 1985.

Thiele, M., Selle, S., Riedel, U., Warnatz, J., Schiessl, R., Maas, U., "A Detailed Two-Dimensional Numerical Study of Spark Ignition Including Ionization", SAE 2002 World Congress, March 2002.

Topinka, J., *Knock Behavior of a Lean-Burn, Hydrogen-Enhanced Engine Concept*, MIT M.S. Thesis in Mechanical Engineering, September 2003.

Tully, E. J., *Lean-Burn Characteristics of a Gasoline Engine Enriched with Hydrogen from a Plasmatron Fuel Reformer*, MIT M.S. Thesis in Mechanical Engineering, June 2002.

Table 1. Reaction Ignition Time (s) due to Radicals Presence

Dissociation	Species Molar Fraction	Ignition Time (s)	
		Ti = 500 K	Ti = 1,000 K
10% O_2	x O = 2.8%	10	5×10^{-3}
10% CH_3	x H = 2.7%	2	3×10^{-3}
Seed	x OH = 2.8%	3	4×10^{-3}
10% O_2 – 10% CH_3	x O = x H = 2.8%	4×10^{-6}	4×10^{-7}
20% O_2	x O = 2.8%	1×10^{-5}	1×10^{-6}
20% CH_3	x H = 2.7%	2×10^{-5}	3×10^{-6}

Table 2. Turbulent Kinetic Energy Estimated from the Input Air and Fuel Stream Jets.

	Atomizer Jet	Wall Air Jet	Swirl Air Jet
No. of orifices	1	2	6
Inlet diameter (mm)	2.5	2.5	2.5
Mass Flow Rate (g/s)	0.84	1.94	1.94
Density (kg/m^3)	0.65	1.2	1.2
Velocity (m/s)	155	160	53
Kappa (m^2/s^2)	3.25×10^4	1.27×10^4	1.41×10^4
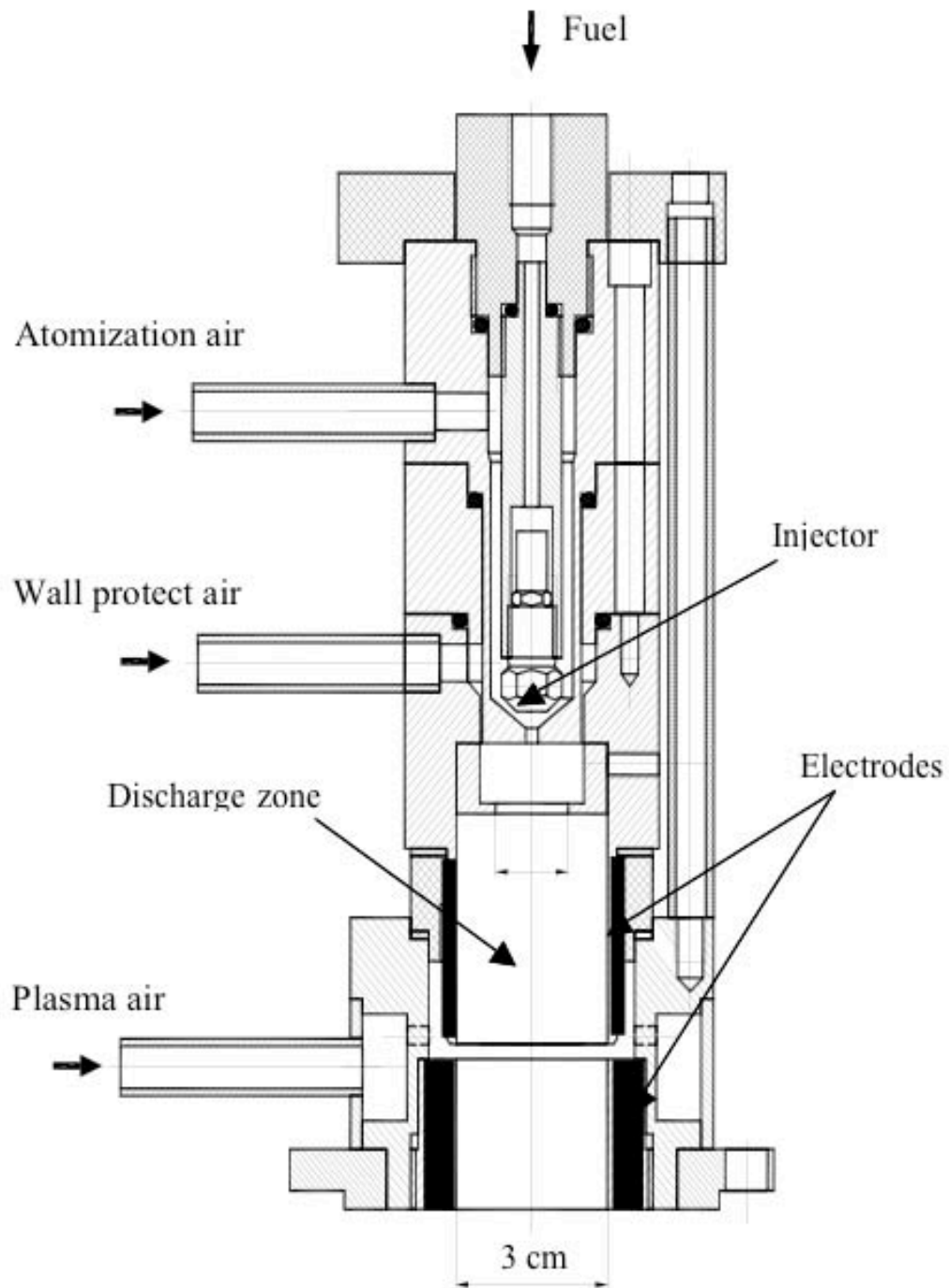
Figure 1. Schematic Drawing of the Plasmatron Design Tested.
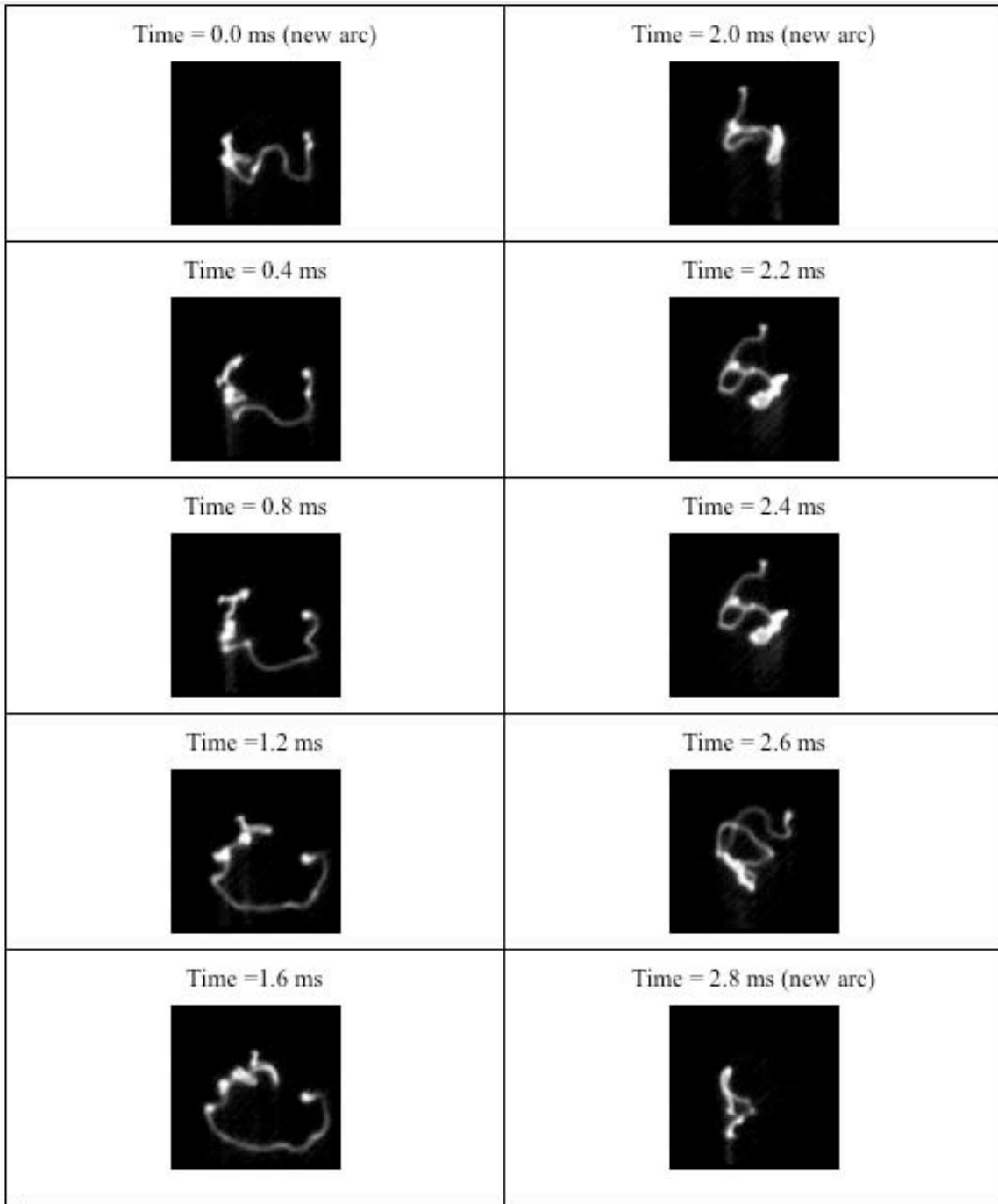
Figure 2. View of the Discharge Region along the y Direction from the Plasmatron Exit. The Sequence of Images along Time includes two Complete Discharges and a Third Arc Initiation
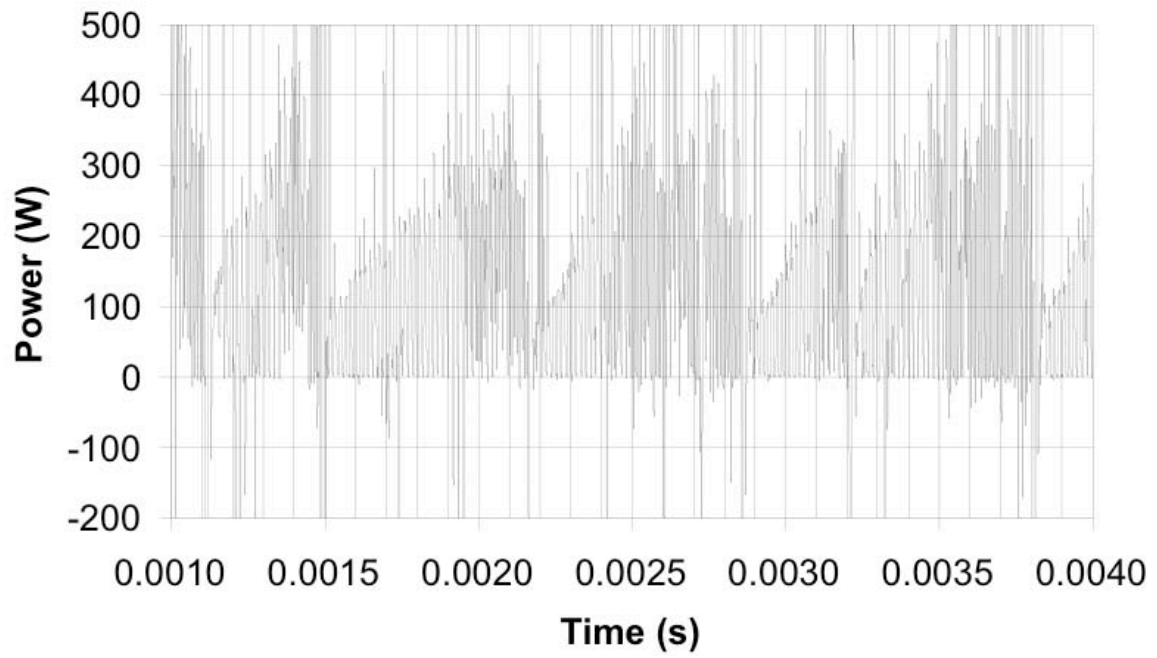
Figure 3. Instantaneous Power Supplied to the Gas Mixture under the Arc along Time.
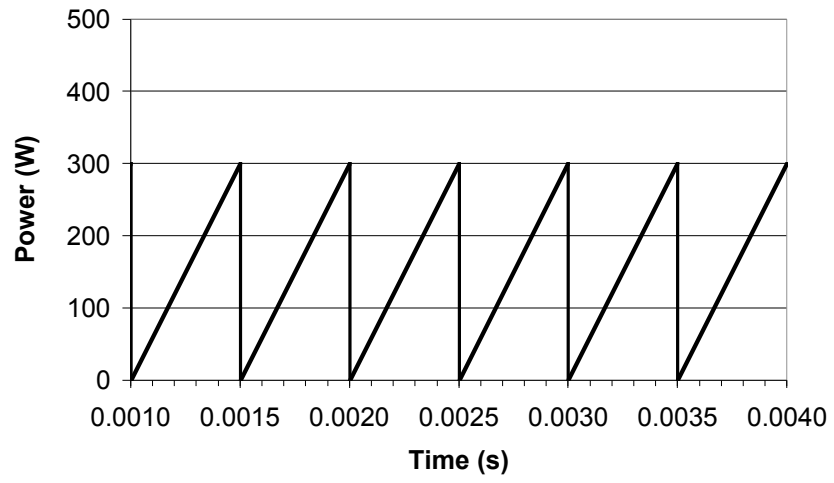
Figure 4. Averaged Power Supplied to the Gas Mixture under the Arc along Time.
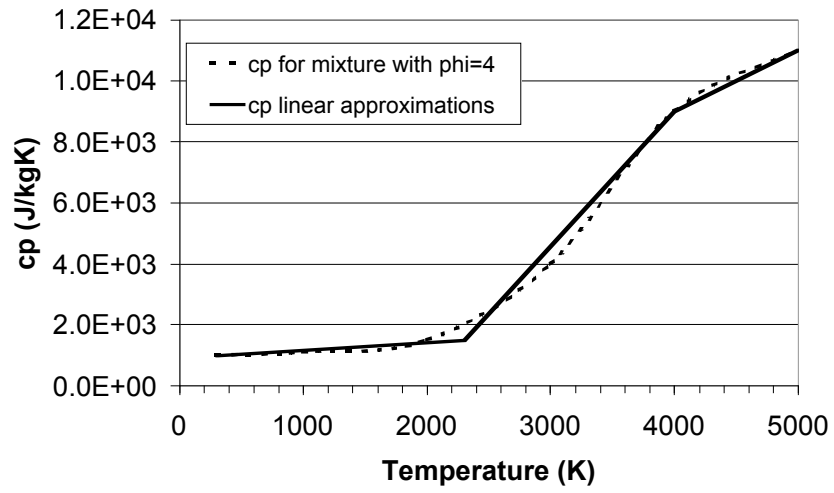
Figure 5. Heat Capacity of the Gas Mixture under the Arc and Linear Approximations.
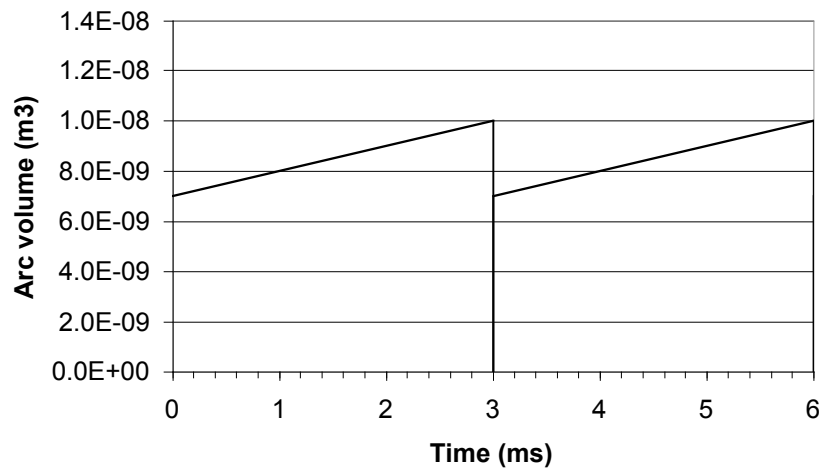
Figure 6. Visually Measured Average Volume of the Arc along Time.
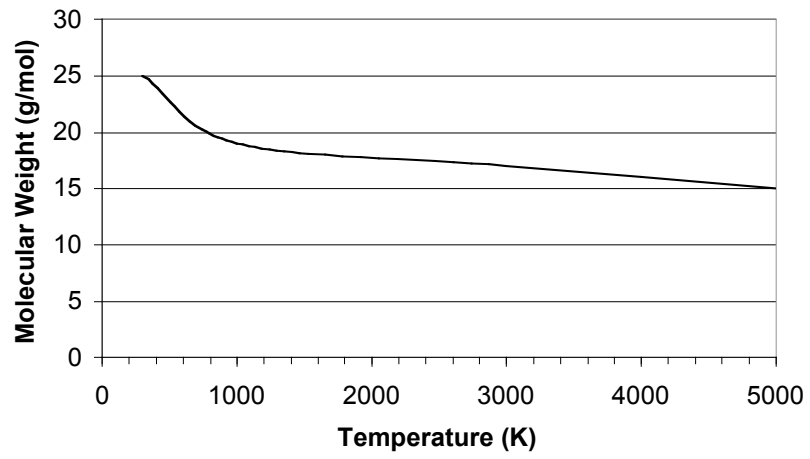
Figure 7. Molecular Weight of the Gas Mixture under the Arc as a Function of Temperature.
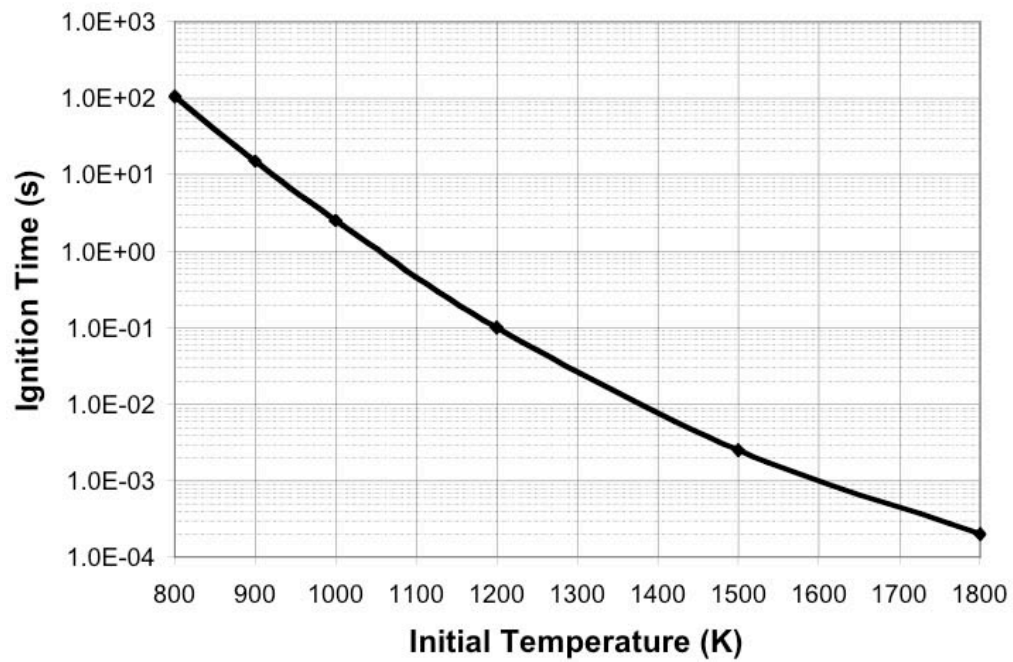
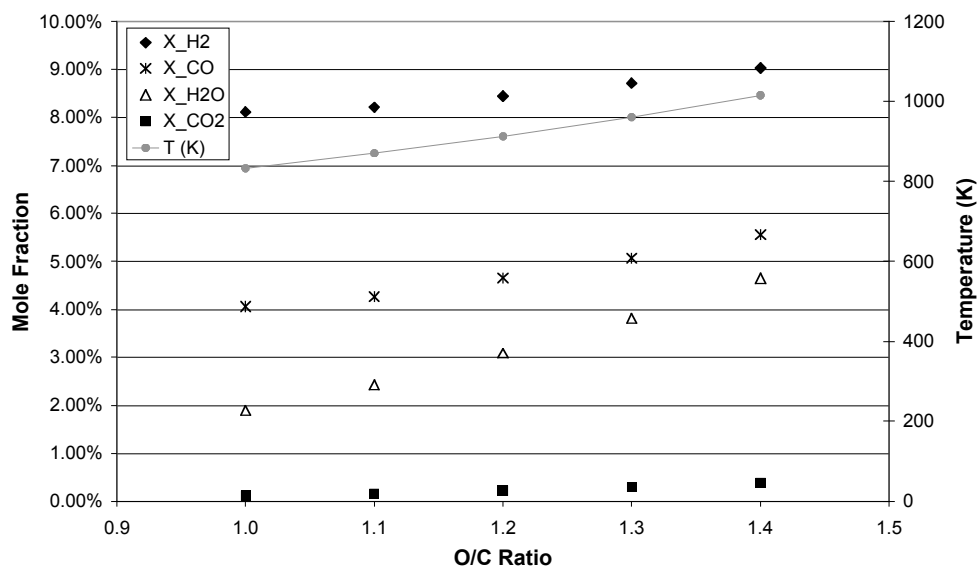Figure 8. Ignition Time as a Function of Initial Temperature in the Plug Flow Reactor O/C=1.

Figure 9. PASR Exhaust Composition for Methane Partial Oxidation using Different O/C, τ_{mix}=0.1 ms and τ_{res}=1 ms, and setting 10% of the Molar Flow at 4,000K Initial Temperature
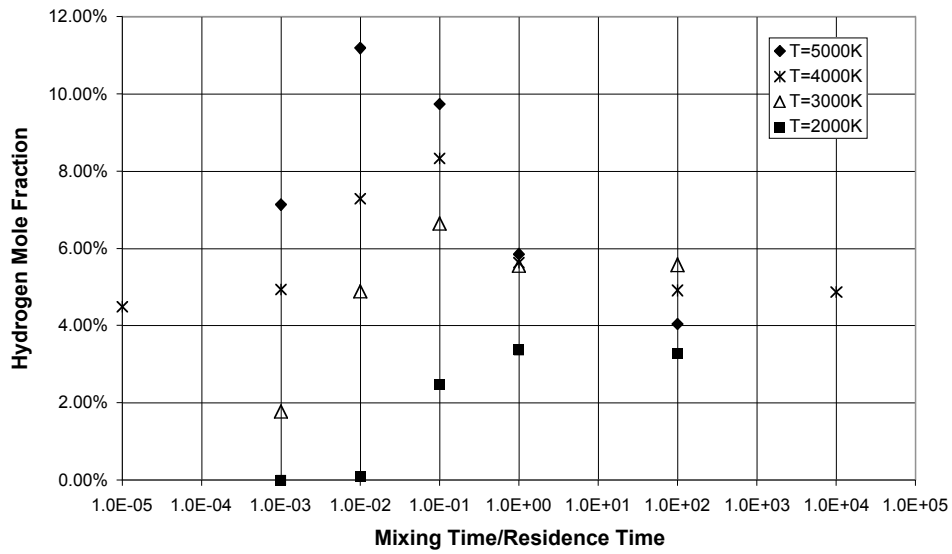
Figure 10. PASR H_2 Exhaust Composition for Methane Partial Oxidation using O/C=1, τ_{res}=1ms and Different τ_{mix}, and setting 10% of the Molar Flow at Different Initial Temperatures.
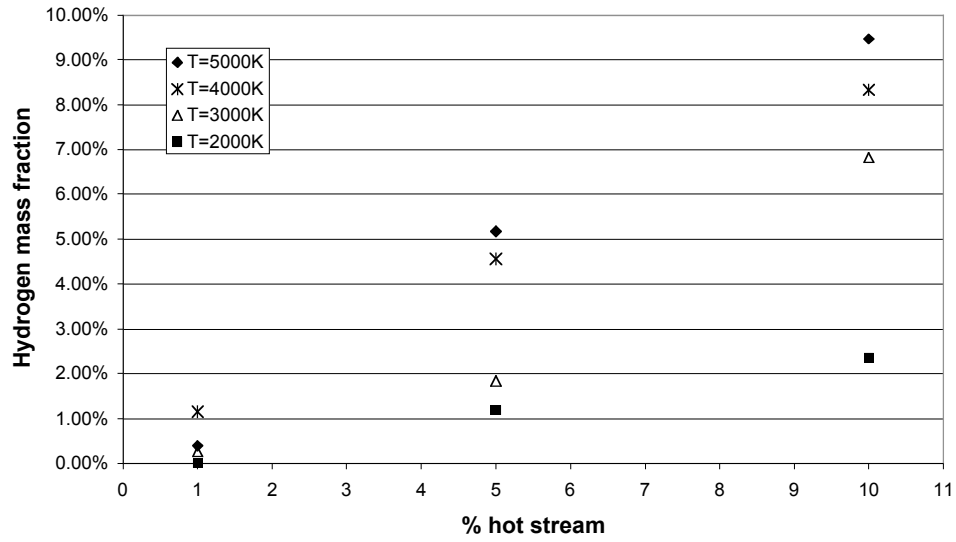
Figure 11. PASR H_2 Exhaust Composition for Methane Partial Oxidation using O/C=1, τ_{res}=1 ms and τ_{mix}=0.1 ms, and setting Different Fractions of the Molar Flow at Different Initial Temperatures.